

Cationic silyldiazenido complexes of the Fe(diphosphine)₂(N₂) platform: structural and electronic models for an elusive first intermediate in N₂ fixation

Received 00th January 20xx,
Accepted 00th January 20xx

DOI: 10.1039/x0xx00000x

www.rsc.org/

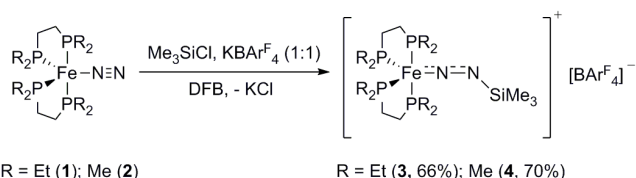
Adam D. Piascik,^a Peter J. Hill,^a Andrew D. Crawford,^a Laurence R. Doyle,^a Jennifer C. Green^b and Andrew E. Ashley^{*a}

The first cationic Fe silyldiazenido complexes, [Fe(PP)₂(NN-SiMe₃)]⁺[BAR^F₄][−] (PP = dmpe/depe), have been synthesised and thoroughly characterised. Computational studies show the compounds to be useful structural and electronic surrogates for the more elusive [Fe(PP)₂(NN-H)]⁺, which are postulated intermediates in the H⁺/e[−] mediated fixation of N₂ by Fe(PP)₂(N₂) species.

The study of well-defined transition metal (TM) species capable of binding and fixing the inert N₂ molecule has been the subject of research for over 50 years, with the last decade seeing increased interest in the use of Fe model complexes as potential nitrogenase mimics.¹ Only a few Fe-containing compounds have been reported that are capable of mediating the catalytic reduction of N₂ using chemical H⁺ and e[−] sources,^{2,3} and we recently reported that the simple Fe(0) phosphine complex Fe(depe)₂(N₂) [**1**; depe = Et₂PCH₂CH₂PEt₂] mediates the efficient catalytic reduction of N₂ in conjunction with excess acid and reductant; this was the first system using a molecular TM compound which was selective for N₂H₄ production over NH₃.⁴ Nevertheless, mechanistic details for these N₂ to N₂H₄/NH₃ conversions remain scarce, mostly due to rapid reaction rates and the high lability of the various FeN_xH_y intermediates.⁵ In particular, examples which establish the structural and electronic changes upon mono-protonation of Fe-ligated N₂ to form diazenide species (Fe-NN-H) remain elusive to date.

Functionalisation of TM-bound N₂ with electrophiles other than H⁺ offers a valuable alternative strategy by which analogues of potential intermediates in the production of NH₃ and N₂H₄ can be isolated. Notably, silylium ions (R₃Si⁺) are valid proton mimics in this regard since they are isolobal and isocharged with H⁺, yet impart an enhanced kinetic stability to

the resultant silyldiazenides, which greatly facilitates the detailed characterisation of complexes relative to their protonated counterparts.^{3,6} However, structurally verified examples resulting from the direct monosilylation of FeN₂ species remain limited^{7–9} and, despite the proven competence of **1** in catalytic N₂ fixation, none have yet been reported for this system.¹⁰ Accordingly, we sought to silylate the coordinated N₂ fragment in **1** and its related congener Fe(dmpe)₂(N₂) (**2**; dmpe = Me₂PCH₂CH₂PMe₂), and herein we report the synthesis and characterisation of the first cationic Fe-silyldiazenido complexes: [Fe(PP)₂(NN-SiMe₃)]⁺ [PP = depe (**3**); dmpe (**4**)]. Furthermore, through the aid of computational calculations, we show that these isolated species emulate the electronic structure of their [Fe(PP)₂(NN-H)]⁺ analogues.



Scheme 1 Synthesis of cationic Fe-silyldiazenido complexes **3** and **4**

Addition of Me₃SiCl¹¹ to solutions of either **1** or **2**¹² in DFB (1,2-difluorobenzene) did not lead to any reaction, as evidenced by ¹H and ³¹P{¹H} NMR spectroscopy. However, subsequent addition of K⁺[BAR^F₄][−] [Ar^F = 3,5-(CF₃)₂C₆H₃; 1 eq.] as a Cl[−] abstracting agent resulted in an immediate colour change to dark red, concomitant precipitation of KCl, and appearance of a new singlet resonance in the ³¹P{¹H} NMR spectrum (δ: 77.0 and 58.6 ppm, from **1** and **2** respectively). After a straightforward work-up, these products were isolated in good yields as dark red, highly air-sensitive microcrystalline solids (Scheme 1) which gave elemental microanalyses consistent with their anticipated composition. Single crystals of each compound suitable for X-ray diffraction were grown from cooled (−30°C) Et₂O solutions, which solved as [Fe(depe)₂N₂(SiMe₃)]⁺[BAR^F₄][−] (**3**) and [Fe(dmpe)₂N₂(SiMe₃)]⁺[BAR^F₄][−] (**4**) (see Figure 1).

^a Department of Chemistry, Imperial College London, Exhibition Road, South Kensington, London SW7 2AZ, UK. E-mail: a.ashley@imperial.ac.uk; Tel: +44 (0) (20) 75945810

^b Inorganic Chemistry Laboratory, University of Oxford, South Parks Rd, Oxford, OX1 3QR, UK.

Electronic Supplementary Information (ESI) available: full experimental details and characterising data. See DOI: 10.1039/x0xx00000x

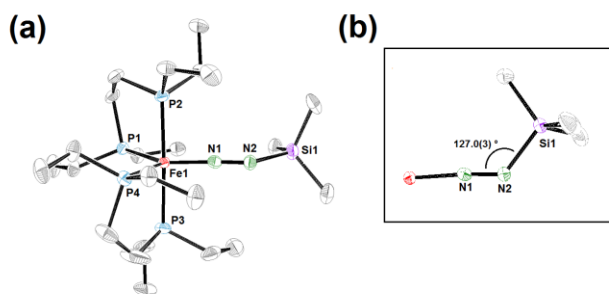


Figure 1. ORTEP diagrams showing the solid-state structures of (a) **3** and (b) an expanded view of Fe-N-N-SiMe₃ unit in **4**, showing acute bending of N-N-Si angle. H atoms and [BAR^F₄][−] counterions omitted for clarity; ellipsoids shown at 50% probability. Refer to Table 1 for selected bond lengths and angles.

4 crystallises with two independent Fe-containing cations in the asymmetric unit, which are virtually identical. **3** and **4** are isostructural and reveal a distorted trigonal bipyramidal geometry about the Fe centre [$\tau = 0.73$ (**3**), 0.79 (**4**)].¹³ The Fe-N bond lengths (see Table 1) are appreciably shorter, and N-N bond lengths notably longer, than in **1** (cf. 1.748(8) Å and 1.142(7) Å respectively);¹⁴ together with the approximately linear Fe-N-N unit this is consistent with Fe-N and N-N π -bonding transmitted along the triatomic framework.

Solution (DFB) IR spectroscopy of **3/4** revealed ν_{NN} values of 1732/1727 cm^{−1} (1669/1668 cm^{−1} for **3-¹⁵N₂/4-¹⁵N₂**) which correspond to substantially weakened N-N bonds in comparison with those found for either **1** or Fe(dmpe)₂(N₂) (IR: 1956 and 1975 cm^{−1}, respectively).¹²

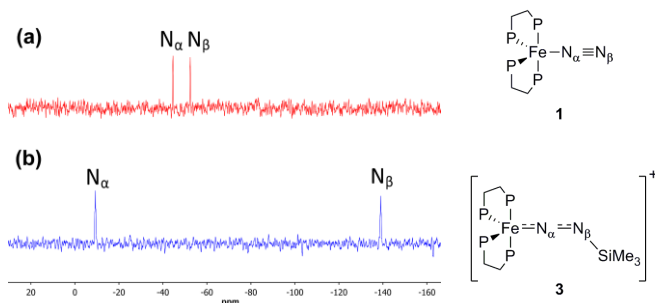


Figure 2. Solution-phase ¹⁵N {¹H} NMR spectra of (a) **1** and (b) **3** (P = PEt₂).

The ¹⁵N{¹H} NMR spectra of ¹⁵N₂-**3/4** (Figure 2) show signals at −9.4/−0.6 ppm (N_α) and −139.1/−130.1 ppm [N_β; verified by ¹H-¹⁵N HMBC spectroscopy to couple with the ¹H resonance of the (CH₃)₃Si group], with the chemical shift differences between N_α and N_β ($\Delta\delta \approx 130$ ppm) being significantly larger than those seen for **1** and **2** ($\Delta\delta = 7.8$ and 1.8 ppm, respectively). The downfield shift for the N_α resonances ($\Delta\delta_{\text{N}_\alpha}$: **3/4** = 35.2/46.4 ppm), and concomitant upfield shift for the N_β signals ($\Delta\delta_{\text{N}_\beta}$: **3/4** = −86.7/−81.3 ppm) from the corresponding values of **1** and **2** are consistent with previously reported changes upon silylation of TM-N₂ species.^{8,15} Collectively these data correlate with an enhanced transfer of electron density from Fe into the NN fragment upon electrophilic attack at the terminal nitrogen (N_β), which results in an increased Fe-N bond order attendant

with a reduction in the N-N bond order. Recently, the borane adduct Fe(depe)₂(NN·B(C₆F₅)₃) has been structurally verified,¹⁶ which permits a valuable comparison between electrophiles of differing Lewis acidity upon the extent of electron transfer from Fe to N₂, using the same parent system **1**. The lower IR stretching frequencies¹⁷ and higher ¹⁵N NMR shift separations seen for **3/4** relative to the B(C₆F₅)₃ compound ($\nu_{\text{NN}} = 1830$ cm^{−1}; $\Delta\delta = 109$ ppm) are consistent with the greater Lewis acidity of [R₃Si]⁺ vs B(C₆F₅)₃,¹⁸ thus translating to augmented Fe→N₂ polarisation and a weaker N-N bond.

Table 1. Experimental and calculated bond lengths and angles for [Fe(PP)₂(N₂-R)]⁺ (R = SiMe₃, H) compounds.

Compound	Fe-N (Å)	N-N (Å)	FeNN (°)	NN(Si/H) (°)
[Fe(depe) ₂ (N ₂ SiMe ₃)] ⁺ 3 ^a	1.691(6)	1.194(8)	171.1(6)	133.8(5)
[Fe(depe) ₂ (N ₂ SiMe ₃)] ⁺ 3 ^b	1.69	1.21	170	138
[Fe(dmpe) ₂ (N ₂ SiMe ₃)] ⁺ 4 ^{a, c}	1.692(3)	1.197(5)	176.2(3)	127.0(3)
	1.692(3)	1.203(5)	175.8(3)	126.9(3)
[Fe(dmpe) ₂ (N ₂ SiMe ₃)] ⁺ 4 ^b	1.69	1.20	173	133
[Fe(depe) ₂ (N ₂ H)] ⁺ 5 ^b	1.68	1.22	175	113
[Fe(dmpe) ₂ (N ₂ H)] ⁺ 6 ^b	1.68	1.22	172	113

[X] = [BAR^F₄][−]. ^a from solid-state X-ray diffraction; ^b determined by DFT calculations (BP86 functional and TZP basis sets, see ESI); ^c two independent cations in asymmetric unit.

The Peters group have reported the structures of five-coordinate *neutral* silyldiazidenes {[o-(PⁱPr₂)C₆H₄]₃E}Fe(NN-SiMe₃) [E = B (**I**), Si (**II**)],^{7,8} which display comparable bond distances (Fe-N, **I/II**: 1.6952(2)/1.6960(8) Å; N-N, **I/II**: 1.225(av)/1.195(3) Å) and IR stretching frequencies (ν_{NN} , **I/II**: 1741/1748 cm^{−1}). These similarities are somewhat surprising considering that the N₂SiMe₃ group in **I/II** is axially bound *trans* to a B/Si atom in contrast to the equatorial site found in **3** and **4**, and the different spin state of **I** ($S = \frac{1}{2}$) vs the diamagnetic nature of **II**, **3** and **4**.

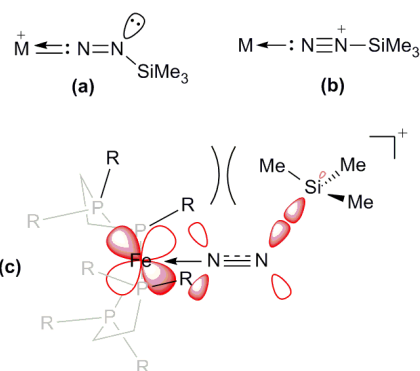


Figure 3. Structures of (a) silyldiazene and (b) silyldiazonium compounds; (c) Fe-N-(SiMe₃) π -bonding description within **3** and **4** (HOMO-1), showing the interplay between electronic and steric effects upon the N-N-SiMe₃ bond angle.

Nevertheless, a key difference between **3/4** and **I/II** are their considerably more acute N-N-Si angles [cf. **I/II**: 164/165.6(3)°],¹⁹ which could indicate lone pair development on N_β (trigonal *sp*² hybridisation) due to significant transfer of

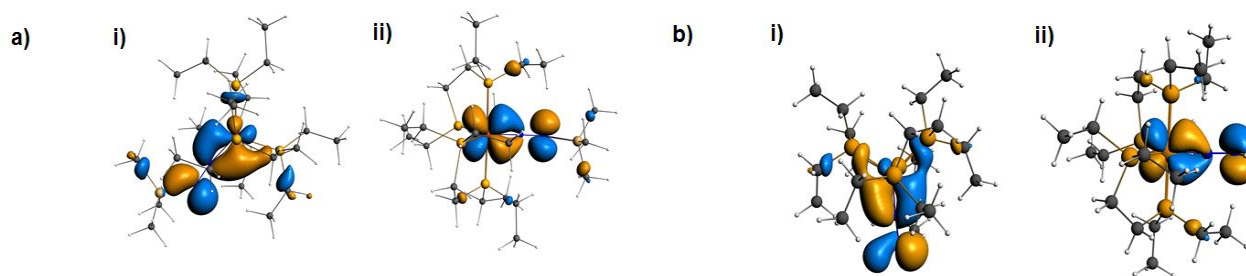


Figure 4. Density functional theory calculated molecular orbitals a) HOMO-1 (i) and HOMO-3 (ii) of **3**; a) HOMO-2 (i) and HOMO-3 (ii) of **5**.

electron density from the Fe centre to $\pi^*(\text{N-N})$.⁷ This could have potential ramifications for the assignment of the *formal* oxidation state of Fe in **3** and **4**. For example, the related complex $\{[o\text{-(PPH}_2\text{C}_6\text{H}_4)_3\text{Si}]\text{Fe}(\text{NN-Ph})\}$ (**III**) shows a N-N-C angle of $122.5(5)^\circ$ (close to that found in **3/4**) and has been described as d^6 Fe(II), whereas the less bent **II** has been formulated as a d^8 Fe(0) anion which backbonds strongly into the π^* orbitals of the $[\text{N}_2\text{SiMe}_3]^+$ fragment;⁸ on the basis of N-N-Si bond angles alone, these suggest that **3** and **4** could be treated as Fe(II) rather than Fe(0) compounds. The structural and electronic features of TM-diazenido compounds has recently been comprehensively reviewed by Dilworth,²⁰ who categorised these latter two examples using a simple valence bond treatment. **III** is termed a ‘singly-bent’ silyldiazenido with the N_2SiMe_3 fragment acting as a $3e^-$ donor (LX; N_β sp^2 hybridised), whilst **II** is considered a rare example of a silyldiazenium adduct which displays a linear TM-N-N-Si geometry and the positively charged ligand donating $2e^-$ (L; N_β sp hybridised) (see Figure 3a and 3b).

In order to gain deeper insight into the electronic structure of the complexes **3** and **4**, density functional theory (DFT) calculations were performed. Geometry optimisation of $[\text{Fe}(\text{PP})_2(\text{NN-SiMe}_3)]^+$ (PP = depe, dmpe) cations gave bond metrics in good agreement with those found experimentally (Table 1; see ESI for full details), although with slightly more obtuse N-N-Si bond angles than those observed from X-ray diffraction data. Whilst the HOMO and HOMO-2 of **3** and **4** are essentially non-bonding on Fe, the HOMO-1 and HOMO-3 of these species display significant Fe-N π -bonding character, indicative of multiple bonding between Fe and N_α (see Figure 4(a) and ESI). To ascertain the degree of population of the N_2SiMe_3 π^* orbitals, calculations were performed on separated $[\text{Fe}(\text{PP})_2]^+$ and N_2SiMe_3 fragments.²¹ These revealed that the N-N π^* orbitals (LUMO and SOMO) are significantly occupied (the N_2SiMe_3 fragment bearing *ca* $-0.15 e^-$ charge) whilst the $\text{Fe}(\text{PP})_2$ moiety has *ca* $+1.15$ of positive charge spread across it, indicating highly effective back-donation from the latter.

Since the experimental and calculated parameters for $[\text{Fe}(\text{PP})_2(\text{NN-SiMe}_3)]^+$ correlate so well, we investigated whether **3** and **4** represented isolable structural and electronic models for their hitherto unobserved $[\text{Fe}(\text{PP})_2(\text{NN-H})]^+$ counterparts. Encouragingly, DFT calculations performed on $[\text{Fe}(\text{PP})_2(\text{NN-H})]^+$ [PP = depe (**5**); dmpe (**6**)²²] provided analogously distorted trigonal bipyramidal geometries ($\tau = 0.81$) and very similar bond metrics to those of $[\text{Fe}(\text{PP})_2(\text{NN-}$

$\text{SiMe}_3)]^+$ (see ESI and Table 1); the four highest energy HOMOs and two lowest energy LUMOs display virtually identical Fe-NNR bonding characteristics to **3** and **4**. Thus, it would appear that isolable **3** and **4** are indeed close mimics of **5** and **6**, which are postulated to be the first intermediates along the pathway to N_2 fixed products upon protonation of the respective $\text{Fe}(\text{PP})_2(\text{N}_2)$ species. Interestingly, the slightly greater elongation of the N-N bond and more acute N-N-R angle found for **5/6** suggest a slightly more activated N_2 unit; this is supported by the enhanced negative charge on the N_2H fragment (*ca* -0.29), and respective positive charge residing on $\text{Fe}(\text{PP})_2$ (*ca* $+1.29$), from fragment calculations.

Szymczak has proposed that the energy of a π^* orbital in N_2 can be lowered *via* interaction with B-based electrophiles, which leads to augmented back-bonding from a $\text{Fe}(\text{depe})_2$ fragment. Using a Walsh-type analysis, it was shown that this interaction is optimised for a bent rather than linear N-N-B bond angle, as this maximises overlap between the B p -orbital and a lobe of the N_2 π^* MO; for the $\text{B}(\text{C}_6\text{F}_5)_3$ adduct this was experimentally determined to be $137.0(3)^\circ$.¹⁶ The experimental and theoretical trends in N-N-R bond angles for the $[\text{Fe}(\text{PP})_2(\text{NN-R})]^+$ species appear to corroborate this theory, demonstrating the greater ability of H^+ to achieve optimal N_2 π^* overlap without leading to the steric penalties encountered by the considerably bulkier Me_3Si^+ group [or indeed $\text{B}(\text{C}_6\text{F}_5)_3$], coupled with the higher electronegativity of H vs Si ($\chi_P = 2.1$ and 1.9 , respectively); together these factors lead to more acute N-N-R angles in **5/6** vs **3/4** commensurate with amplified $\text{Fe} \rightarrow \text{N}_2$ polarisation. Thus, this series of compounds, which probe how different electrophiles affect the extent of N_2 activation in closely related $\text{Fe}(\text{PP})_2(\text{N}_2)$ systems, also reveals a correlation with N-N-R bending which is an interplay between the steric requirements and the electrophilicity of the R group (see Figure 3c).

Notably for all $[\text{Fe}(\text{PP})_2(\text{NN-R})]^+$ complexes examined here, the highest occupied orbitals have significant $3d$ content, and hence the trigonal bipyramidal structure characteristic of a five-coordinate d^8 FeL_5 system [e.g. $\text{Fe}(\text{CO})_5$]. In conjunction with the diamagnetic behaviour of **3** and **4**, these results suggest that their bonding is best described akin to that in **II** *viz.* a low-spin neutral Fe(0) $\text{Fe}(\text{PP})_2$ fragment which exhibits potent back-bonding and charge transfer into the $2e^-$ donor ligand $[\text{N}_2\text{SiMe}_3]^+$, that ultimately renders the $\text{Fe}(\text{PP})_2$ core as the principal acceptor of positive charge.

Conclusions

The direct silylation of the terminal N atom in $\text{Fe}(\text{PP})_2(\text{N}_2)$ (PP = depe, dmpe) has enabled the synthesis and structural characterisation of $[\text{Fe}(\text{PP})_2(\text{N}_2\text{-SiMe}_3)][\text{BAR}^{\text{F}}_4]$, the first cationic Fe species containing a silylated diazenido ligand, which feature substantial N-N bond weakening and unusually acute N-N-SiMe₃ bond angles. Computational investigations show these formally $\text{Fe}(0)$ d^8 species are effective structural and electronic mimics of the hitherto non-isolable $[\text{Fe}(\text{PP})_2(\text{N}_2\text{-H})]^+$, postulated first intermediates in N_2 fixation by protonation of $\text{Fe}(\text{PP})_2(\text{N}_2)$, thus validating the hypothesis that the $[\text{SiMe}_3]^+$ group is an instructive structural and electronic surrogate for H^+ . Further investigations into the use of silylated analogues to probe the mechanism of N_2 fixation by $\text{Fe}(\text{PP})_2(\text{N}_2)$ are now underway.²³

Notes and references

- 1 N. Hazari, *Chem. Soc. Rev.*, 2010, **39**, 4044; K. C. MacLeod and P. L. Holland, *Nat. Chem.*, 2013, **5**, 559; B. A. MacKay and M. D. Fryzuk, *Chem. Rev.*, 2004, **104**, 385.
- 2 J. S. Anderson, J. Rittle and J. C. Peters, *Nature* 2013, **501**, 84; S. E. Creutz and J. C. Peters, *J. Am. Chem. Soc.* 2014, **136**, 1105; T. J. Del Castillo, N. B. Thompson and J. C. Peters, *J. Am. Chem. Soc.* 2016, **138**, 5341; S. Kuriyama, K. Arashiba, K. Nakajima, Y. Matsuo, H. Tanaka, K. Ishii, K. Yoshizawa and Y. Nishibayashi, *Nat. Commun.*, 2016, **7**, 12181; M. J. Chalkley, D. J. Del Castillo, B. D. Matson, J. P. Roddy and J. C. Peters, *ACS Cent. Sci.* 2017, **3**, 217.
- 3 G. Ung and J. C. Peters, *Angew. Chem. Int. Ed.*, 2015, **54**, 532;
- 4 P. J. Hill, L. R. Doyle, A. D. Crawford, W. K. Myers and A. E. Ashley, *J. Am. Chem. Soc.*, 2016, **138**, 13521.
- 5 J. S. Anderson, G. E. Cutsail III, J. Rittle, B. A. Connor, W. A. Gunderson, L. Zhang, B. M. Hoffman and J. C. Peters, *J. Am. Chem. Soc.*, 2015, **137**, 7803; J. Rittle and J. C. Peters, *J. Am. Chem. Soc.*, 2016, **138**, 4243; J. Rittle and J. C. Peters, *J. Am. Chem. Soc.* 2017, **139**, 3161.
- 6 M. Hidai, K. Komori, T. Kodama, D. Jin, T. Takahashi, S. Sugiura, Y. Uchida and Y. Mizobe, *J. Organomet. Chem.*, 1984, **272**, 155.
- 7 M. Moret and J. C. Peters, *J. Am. Chem. Soc.*, 2011, **133**, 18118.
- 8 Y. Lee, N. P. Mankand, J. C. Peters, *Nat. Chem.*, 2010, **2**, 558.
- 9 J. Rittle and J. C. Peters, *Proc. Natl. Acad. Sci. U.S.A.*, 2013, **110**, 15898.
- 10 Field *et al.* have reported that *in situ* reactions of **2** with Me_3SiOTf in hexane generates mixtures of *trans*- $[\text{H-Fe}(\text{N}_2)(\text{dmpe})_2]^+$, $[\text{Fe}(\text{dmpe})_3]^{2+}$ (~84% assigned) and presumably an N-trimethylsilylated species. However, attempts to spectroscopically characterise the latter, or any product arising from the combination of Me_3SiOTf and **1**, were unsuccessful. See L. D. Field, N. Hazari and H. L. Li, *Inorg. Chem.*, 2015, **54**, 4768.
- 11 Whilst the more powerful silylating agent Me_3SiOTf led to a broadening of the ^{31}P NMR resonances of **1** and **2**, indicating reversible $\text{N}_\beta\text{-Si}$ bond formation, these solutions were unstable and decomposed to uncharacterised products. Since Me_3SiCl gave clean conversions, we adopted this as the $[\text{Me}_3\text{Si}]^+$ synthon.
- 12 L. R. Doyle, P. J. Hill, G. G. Wildgoose and A. E. Ashley, *Dalton Trans.*, 2016, **45**, 7550. **2** was generated *in situ* from solutions of $[\text{Fe}(\text{dmpe})_2](\mu\text{-N}_2)$ under N_2 .
- 13 $\tau = 0$ or 1 for perfect square-based pyramidal and trigonal bipyramidal geometries, respectively. See A. W. Addison, T. N. Rao, J. Reedijk, J. van Rijn and G. C. Verschoor, *J. Chem. Soc. Dalton Trans.*, 1984, 1349.
- 14 C. Perthuisot and W. D. Jones, *New J. Chem.*, 1994, **18**, 621.
- 15 D. V. Yandulov and R. R. Schrock, *J. Am. Chem. Soc.*, 2002, **124**, 6252-6253.
- 16 J. B. Geri, J. P. Shanahan and N. K. Szymczak, *J. Am. Chem. Soc.*, 2017, **139**, 5952.
- 17 It has been shown that ν_{NN} is a more reliable estimate of N_2 bond strength/activation than N-N bond lengths from solid-state X-Ray crystallographic data. See ref. 1 and P. Müller, *Crystallogr. Rev.*, 2009, **15**, 57.
- 18 H. Großekappenberg, M. Reißmann, M. Schmidtman and Thomas Müller, *Organometallics* 2015, **34**, 4952.
- 19 Peters *et al.* have reported Fe-bound monosilylated diazenido fragments with comparably acute N-N-Si angles: $[(\text{P}_3\text{B})\text{Fe}(\text{NN-SiMe}_3)]\text{Na}(\text{THF})$ ($\text{P} = o\text{-(P}^i\text{Pr}_2)_2\text{C}_6\text{H}_4$)⁷ and $[\text{C}^{\text{Si}}\text{P}^{\text{Ph}}_3]\text{Fe}(\text{NN-Si}^i\text{Pr}_3)$ ⁹ [$\text{C}^{\text{Si}}\text{P}^{\text{Ph}}_3 = (\text{Ph}_2\text{PCH}_2\text{SiMe}_2)_3\text{CH}$] ($\text{N-N-Si} = 131.3(2)^\circ$ and 135.11° , respectively). Note, however, that in each case their synthesis proceeds with substantial rearrangement of the metal coordination sphere from a trigonal bipyramidal geometry of the starting material. In the former the Na cation displays η^2 -binding to the N-N fragment and an aryl ring, while for the latter dechelation of a phosphine arm results in a pseudo-tetrahedral complex. Accordingly, a straightforward comparison of these species with 5-coordinate FeNNSiR_3 compounds is not possible.
- 20 J. R. Dilworth, *Coord. Chem. Rev.*, 2017, **330**, 53.
- 21 The choice of which fragment bore the positive charge had a marginal effect on the calculations, but given that the $\text{Fe}(\text{PP})_2$ moiety carries a positive charge in the final result it seemed the more logical bearer of charge in the fragment form. These fragments retained the geometry they possessed in the parent cation, using their MOs as the basis set rather than AOs. See ESI for more details.
- 22 The bond lengths and angles for **6** are reassuringly similar to those reported in a theoretical study of N_2 reduction to NH_3 by $\text{Fe}(\text{dmpe})_2(\text{N}_2)$: R. B. Yelle, J. L. Crossland, N. K. Szymczak, D. R. Tyler, *Inorg. Chem.* 2009, **48**, 861.
- 23 The thermally unstable diamagnetic complex $\{\text{Fe}(\text{depe})_2[\text{NN}(\text{H})\cdot\text{B}(\text{C}_6\text{F}_5)_3]\}^+$ has been previously isolated from the reaction of $[\text{H}(\text{OEt})_2]_2^+[\text{BAR}^{\text{F}}_4]^-$ with $\text{Fe}(\text{depe})_2(\text{NN}\cdot\text{B}(\text{C}_6\text{F}_5)_3)$. Identical protonation reactions of **3**, however, form paramagnetic solutions whose colour differed under Ar (blue) or N_2 (yellow), which is characteristic of $\text{Fe}(\text{I})$ -bisphosphine complexes (see ref. 16 and C. G. Balesdent, J. L. Crossland, D. T. Regan, C. T. Lopez and D. R. Tyler, *Inorg. Chem.*, 2013, **52**, 14178). We are currently investigating this divergent reactivity.